FEATURES OF METHANE EMISSION IN COAL MINES AT HIGH SPEED LONGWALL FACE ADVANCE

Skipochka S.I.
Institute of Geotechnical Mechanics named by N. Poljakov of National Academy of Sciences of Ukraine, Professor, Doctor of Technical Sciences, Head of Laboratory of Physics and Geomechanical Monitoring of Rock Massif, Ukraine

Krukovskyi O.P.
Institute of Geotechnical Mechanics named by N. Poljakov of National Academy of Sciences of Ukraine, Corresponding member of NAS of Ukraine, Doctor of Technical Sciences, Deputy Director of the Institute, Ukraine

Krukovska V.V.
Institute of Geotechnical Mechanics named by N. Poljakov of National Academy of Sciences of Ukraine, Senior Researcher, Doctor of Technical Sciences, Senior Researcher in Department of Dynamic Effects of Rock Pressure Control, Ukraine

Palamarchuk T.A.
Institute of Geotechnical Mechanics named by N. Poljakov of National Academy of Sciences of Ukraine, Doctor of Technical Sciences, Principal Researcher in Laboratory of Physics and Geomechanical Monitoring of Rock Massif, Ukraine

Abstract. The increase in coal mining is constrained by the gas factor. At high speed of wall advance, the current standards for the forecast of methane emission give significant errors. The goal of work is to study features of methane emission in coal mines at high speed longwall face advance.

The proposed method takes into account the geomechanics of the filtration region formation in the calculation of methane inflow. The method consists in sequential calculation of geomechanical parameters, rock permeability coefficients and methane filtration parameters. Established that the step of landing the main roof increases linearly with increasing speed of longwall advance. The blocks size increases and the fracturing rocks decreases. The size of the filtration area is reduced near the working stope. The front boundary of the filtration area moves closer to the longwall face.

Remote sources of gas emission go beyond the filtration area. The residual pressure of methane increases in undermined gas-bearing rocks and coal. The process of destruction and the emission of electrons decreases. This leads to a slowdown in methane desorption processes.

Thus, an increase in the speed of wall advance allows to reduce specific gas emission in the production sites. However, the requirements for the powered roof and drift supports are increasing due to the increase and redistribution of stresses in the rocks. This should be taken into account when choosing the optimal operating conditions for the mining section of a coal mine.

Key words: longwall, wall advance, geomechanical processes, gas dynamics, methane emission, desorption.

1 Introduction

During the design, the expected methane abundance of the mining sites is determined from the methane content of the coal seams and the host rocks. As a rule, their natural methane content for existing mines is determined by exploration data. Actual methane emissions are calculated by the mine ventilation service based on measurements of air flowrate and gas concentration.

Over the past 10-15 years, Ukrainian mines have switched to intensive coal mining technologies. Longwall average load was increased by 3-5 times. The requirements for monitoring the mine atmosphere were tightened. Analysis of the control results showed that with loads on the working face of more than 3 thousand tons/day, the forecast and control data differ significantly [1, 2]. Therefore, at the wall advance speed of more than 6 m/day, an uncertain situation occurs, which can lead to a decrease in mining safety. The reason for this phenomenon is rocks stress redistribution, rock deformation, and methane filtration. To date, research in this area has been episodic.

The goal of this work is to study features of methane emission in coal mines at high speed of the wall advance.

The objectives of the study included: determining the effect of the rate of mining on geomechanical processes in the rock massif; studying the mechanism of formation of the filtration area and determining the dependence of permeability on the rocks stress state; establishing the dependence of changes in the flowrate of methane into the lava at various speeds of its movement.

2 Methods

The problem was solved using analytical research methods based on continuum mechanics, elasticity theory, gas dynamics, and material resistance methods.

The methane filtration process in disturbed rocks in the zone of influence of the mine working was studied by the method of numerical three-dimensional modeling.

The methodology for studying the process of gas evolution from the host rocks into the mine workings included: calculation of geomechanical parameters; calculation of rock permeability coefficients depending on the components of the principal stress tensor; calculation of filtration parameters (methane pressure, filtration rate, methane flowrate).

The results were analyzed and summarized.

3 Results and discussion

3.1 The influence of the speed of longwall face advance on geomechanical processes in a rock massif

It is known that the dominant factor of geomechanical processes in the "longwall – rock massif" system is the formation of a rock console (plate) hanging over the waste [3]. Moreover, the increase in the speed of the movement of the coal face leads to an increase in the size of this console.

Let us evaluate the changes in the magnitude of the load on the clamping area of the rock-roof console. To simplify the calculations, we neglect the secondary features in the kinematics of the phenomenon under consideration. Since we are interested in the bending of the plate, we accept the hypothesis of direct normals. Therefore, when solving the problem, we use the following assumptions:

- until the plate is deformed, the set of points lying on a straight line normal to the elastic median plane remains on the straight line normal to the elastic deformation surface;
- the σ_{zz} component is small in comparison with other components of the stress tensor;
- when the plate is bent, the median plane is not deformed.

With these assumptions, we write the differential equation for the elastic surface of a curved plate in the form

$$\frac{Eh_p^{\,3}}{12(1-\nu^2)}\left(\frac{\partial^4 u}{\partial x^4}+2\frac{\partial^2 u}{\partial x^2}\frac{\partial^2 u}{\partial y^2}+\frac{\partial^4 u}{\partial y^4}\right)=q, \qquad (1)$$

where E is Young's modulus of elasticity, Pa; h_p is plate thickness, m; ν is plate Poisson's ratio; u is displacement, m; q is load intensity distributed evenly, N/m.

Let the plate be clamped by the load per unit length evenly distributed along the edges $y = 0$ (Fig. 1).

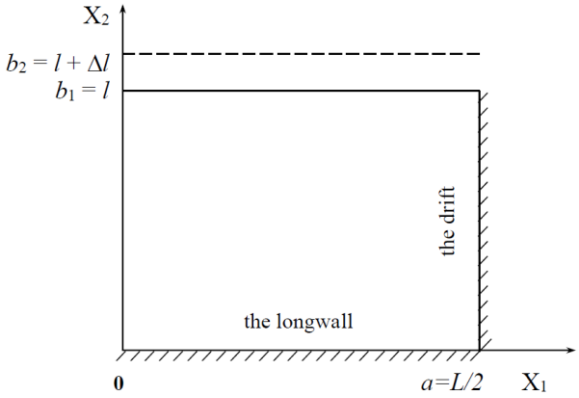

Fig. 1. The scheme for calculating the change in the magnitude of the load in the destruction zone of the face roof

We set the equation of the elastic surface in the form

$$u=\sum_{k=1}^{\infty}\sum_{n=1}^{\infty}A\sin\frac{k\pi x_1}{a}\sin\frac{n\pi x_2}{b}, \qquad (2)$$

where A is maximum displacement, m; a, b is plate length and width, m.

The displacement of the plate u and the speed of its displacement must satisfy the boundary conditions, which depend on the method of fixing the plate, and the initial conditions:

$$u=u_0(x_1,x_2); \quad \frac{\partial u}{\partial t}=v_0(x_1,x_2) \text{ for } t=0,$$

where u_0 is starting point (x_1, x_2) offset, m; v_0 is initial set speed at a point (x_1, x_2), m/day.

Let us consider the main roof with a thickness h_r in the form of a plate $h_r=h_p$, fixed on two adjacent sides a and b. The solution of equation (1) by the Runge-Kutta method in general is written as follows

$$\omega^2 = \frac{\pi^2 \delta}{a^2}\sqrt{\frac{D}{M^*}},$$

where $D = \frac{Eh_r^{\,3}}{12(1-\nu^2)}$ is plate bending stiffness, N/m; $M^* = \rho h_r$ is plate weight per unit area, kg/m^2; ρ is roof rock density, kg/m^3; δ is coefficient of the type of jamming of the roof contour.

For a plate with two adjacent rigidly fixed and two free sides, the circular frequency of its own oscillations is equal to:

$$\omega = 3{,}518\sqrt{\frac{1}{a^4} + (3{,}493 - 3{,}374\nu)\frac{1}{a^2 b^2} + \frac{1}{b^4}} \cdot \sqrt{\frac{D}{M^*}}. \qquad (3)$$

Given $\omega = 2\pi f$ and the velocity of the longitudinal acoustic wave in the plate is equal to

$$c_p = \sqrt{\frac{E}{\rho(1-\nu^2)}},$$

we rewrite formula (3) in the form

$$f = 0{,}145 h_p c_p \sqrt{\frac{1}{a^4} + (3{,}493 - 3{,}374\nu)\frac{1}{a^2 b^2} + \frac{1}{b^4}}.$$

The equations for determining bending moments are written as follows

$$M_{x_1} = -D\left(\frac{\partial^2 u}{\partial x_1^2} + \nu\frac{\partial^2 u}{\partial x_2^2}\right); \quad M_{x_2} = -D\left(\frac{\partial^2 u}{\partial x_2^2} + \nu\frac{\partial^2 u}{\partial x_1^2}\right);$$

$$M_{x_1 x_2} = -M_{x_2 x_1} = D(1-\nu)\frac{\partial^2 u}{\partial x_1 \partial x_2}.$$

Substituting solution (2) into these equations, we obtain for the values of the maximum bending moment

$$M_{x1} = \frac{\zeta a^2 b^2 (a^2 + \nu b^2)\pi^2 \rho {h_p}^3}{b^4 + (3{,}493 - 3{,}374\nu)a^2 + a^4} \sin\frac{k\pi x_1}{a} \sin\frac{n\pi x_2}{b};$$

$$M_{x2} = \frac{\zeta a^2 b^2 (b^2 + \nu a^2)\pi^2 \rho {h_p}^3}{b^4 + (3{,}493 - 3{,}374\nu)a^2 + a^4} \sin\frac{k\pi x_1}{a} \sin\frac{n\pi x_2}{b}. \quad (4)$$

For the case in question ζ = 0,245. Support reactions at the edges of the plates are equal to

$$R_{x1} = \left(Q_{x1} - \frac{\partial M_{x1x2}}{\partial x_2} \right); \qquad R_{x2} = \left(Q_{x2} - \frac{\partial M_{x1x2}}{\partial x_1} \right), \quad (5)$$

where Q_{x1} и Q_{x2} is values of cutting forces N equal to:

$$Q_{x1} = \frac{\partial M_{x2x1}}{\partial x_2} + \frac{\partial M_{x1}}{\partial x_1} = -D\frac{\partial}{\partial x_1}\left(\frac{\partial^2 u}{\partial x_1^2} + \frac{\partial^2 u}{\partial x_2^2} \right);$$

$$Q_{x2} = \frac{\partial M_{x2}}{\partial x_2} - \frac{\partial M_{x1x2}}{\partial x_1} = -D\frac{\partial}{\partial x_2}\left(\frac{\partial^2 u}{\partial x_1^2} + \frac{\partial^2 u}{\partial x_2^2} \right). \quad (6)$$

In view of equations (4)-(6), the support reactions fixed at the edges of the plate are equal to

$$R_{x1} = \frac{\gamma h_p}{\pi a\left[\frac{1}{a^4} + (3{,}493 - 3{,}374\nu)\frac{1}{a^2 + b^2} + \frac{1}{b^4} \right]} \left(\frac{1}{a^2} + \frac{2-\nu}{b^2} \right)^2 \sin\frac{\pi x_2}{b};$$

$$R_{x2} = \frac{\gamma h_p}{\pi b\left[\frac{1}{a^4} + (3{,}493 - 3{,}374\nu)\frac{1}{a^2 + b^2} + \frac{1}{b^4} \right]} \left(\frac{1}{b^2} + \frac{2-\nu}{a^2} \right)^2 \sin\frac{\pi x_1}{a}.$$

The resulting reaction will be expressed as

$$R = \frac{2\gamma h_p}{\pi\left[\frac{1}{a^4} + (3{,}493 - 3{,}374\nu)\frac{1}{a^2 + b^2} + \frac{1}{b^4} \right]} \left[\frac{1}{a}\left(\frac{1}{a^2} + \frac{2-\nu}{b^2} \right) \right].$$

$$\cdot\int_0^b \sin\frac{\pi x_2}{b}dx_2 + \frac{1}{b}\left(\frac{1}{b^2}+\frac{2-\nu}{a^2}\right)\int_0^a \sin\frac{\pi x_1}{a}dx_1\Bigg] =$$

$$= \frac{4\gamma h_p}{\pi^2}\left\{ab + \frac{2(1-\nu)}{ab\left[\frac{1}{a^4}+(3{,}493-3{,}374\nu)\frac{1}{a^2+b^2}+\frac{1}{b^4}\right]}\right\}.$$

Let us evaluate how the load will change when the roof length is equal to half the length of the longwall face ($a=L/2$), and change b within $l \le b \le l+\Delta l$. Then, with $b=l$ and $h_p=h_r$

$$R^{\text{I}} = \frac{4\gamma h_r}{\pi^2}\left\{\frac{Ll}{2} + \frac{2(1-\nu)}{\frac{Ll}{2}\left[\frac{16}{L^4}+(3{,}493-3{,}374\nu)\frac{4}{L^2l^2}+\frac{1}{l^4}\right]}\right\}.$$

At $b = l + \Delta l$

$$R^{\text{II}} = \frac{4\gamma h_r}{\pi^2}\cdot\left\{\frac{L(l+\Delta l)}{2} + \frac{2(1-\nu)}{\frac{L(l+\Delta l)}{2}\left[\frac{16}{L^4}+(3{,}493-3{,}374\nu)\frac{4}{L^2(l+\Delta l)^2}+\frac{1}{(l+\Delta l)^4}\right]}\right\}.$$

Neglecting the terms of the second order of smallness, we obtain

$$\Delta R \approx \frac{4\gamma h_r \Delta l}{\pi^2}\left\{\frac{L}{2} + \frac{4(1-\nu)}{Ll(l+\Delta l)\left[\frac{16}{L^4}+(3{,}493-3{,}374\nu)\frac{4}{L^2l^2}+\frac{1}{l^4}\right]}\right\}.$$

From the expression it follows that the increment of the load at the point of clamping the face roof is directly proportional to the increment of its length, power, and also the speed of longwall movement (Fig. 2).

In addition, there are changes in the electrodynamics of the process. Electron emission decreases due to a decrease in the surface area of the resulting cracks [4, 5]. The energy of these electrons is sufficient to activate methane molecules bound by the Van der Waals forces. Consequently, the process of methane desorption with an in-

crease in the speed of movement of the longwall face also slows down.

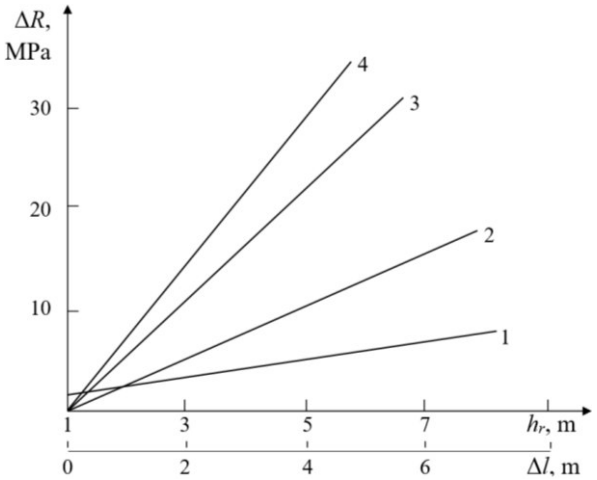

Fig. 2. The dependence of the increment of the load on the clamp of the roof on its thickness (*1*) and increase the length of the console when: *2* – h_r=2 m, *3* – h_r=4 m, *4* – h_r=6 m

Summarizing, we can draw the following conclusions.

1. In a transversely isotropic rock massif, the length of the longwall roof console is directly proportional to its thickness and elastic modulus of rocks, inversely proportional to the depth of mining and the degree of heterogeneity of the massif, it increases linearly with increasing speed of the face

2. In unstable and medium-stable rocks, with an increase in the speed of movement of the longwall from 0 to 12 m/day, the fall step of the main roof increases from 15-17 to 25-28 m.

3. With an increase in the speed of movement of longwall face due to a decrease in the intensity of formation of cracks, the methane desorption process slows down. This is due to a decrease in the activation of bound methane molecules by emitting electrons.

3.2 Simulation of methane filtration process

The most general model of a rocks is a fractured-porous, layered, and anisotropic medium within each layer. A gas flow consisting of

air, methane, and other gases we assume a continuous medium that fills the entire fractured-pore space of the massif.

Let's consider the conditions when the longwall moved away from the shaft furnace a sufficient distance and moves at a constant speed. The filtration area moves with the face at the same speed. In this case, the equations of deformation and filtration, boundary and initial conditions remain unchanged [6]. Therefore, we consider this processes as steady in a moving coordinate system associated with a moving longwall face.

Methane in sandstones and coal is in free and bound states [7, 8]. Thus, the methane desorption and its decay property in time have a significant effect on the filtration process. Methane desorption from disturbed coal seams and gas-bearing sandstones can be represented as the uniformly distributed methane sources $q(t)$. In the case of gas desorption from a coal seam, we assume that

$$q(t) = q_0 \cdot e^{-at},$$

where q_0 is initial gas emission, m^3/t; a is coefficient of accounting for properties of gas emission from a coal seam, 1/s; t is time from the start of gas emission, s.

Taking into account the speed of the wall advance V_{lw}, m/s, and the distance from the boundary of the filtration area z, m

$$q = q_0 \cdot e^{-a\frac{z}{V_{lw}}}.$$

The calculations take into account that exhaustion of emissions from gas-bearing sandstones occurs 4 times faster [9]. Coupled quasi-stationary three-dimensional processes of the rocks deformation and gas filtration in a disturbed area are described by a system of equations [10, 11]

$$\sigma_{ij,j} + X_i(t) = 0;$$
$$\frac{k}{2m\mu}\left(\frac{\partial^2 p^2}{\partial x^2} + \frac{\partial^2 p^2}{\partial y^2} + \frac{\partial^2 p^2}{\partial z^2}\right) + q(t) = 0;$$

where $\sigma_{ij,j}$ is the derivatives of the stress tensor components along x, y, Pa/m; $X_i(t)$ is the projections of the external forces acting on the

volume unit of a solid body, N/m^3; p is the gas pressure, Pa; k is the permeability coefficients, D; m is porosity; □ is gas viscosity, Pa·s; $q(t)$ is the gas release function.

The boundary conditions for the task set

$$u_x\big|_{\Omega_1} = 0; \quad u_z\big|_{\Omega_1} = 0; \quad u_y\big|_{\Omega_2} = 0;$$

$$p\big|_{\Omega_1} = p_0; \quad p\big|_{\Omega_2} = p_0; \quad p\big|_{\Omega_3} = p_0; \quad p\big|_{\Omega_4} = 0.1 \text{ MPa};$$

where □$_1$, □$_2$ is the vertical and the horizontal boundaries of the outer contours; p_0 is the methane pressure in the virgin rocks, MPa; □$_3$ is the boundary of the filtering area; □$_4$ is the internal contour (the mine working).

The problem is solved in an elastic-plastic formulation. For the mathematical description of the process of rocks changeover into a disturbed state, the Mohr-Coulomb failure theory is applied. To solve the problem, we used the finite element method.

Verification of the gas filtration model in the disturbed area was performed by comparing the calculated data on the gas release into the well with analytical solutions; comparison with experimental data on the distribution of gas pressure around the well and pressure changes in the dig up coal seam. The calculation error did not exceed 15 %.

Geomechanical parameters Q^* and P^* are used to analyze the stress state of rocks. Q^* - the parameter characterizing the diversity of the stress field components; P^* - the parameter characterizing the unloading of rocks from the rock pressure

$$Q^* = \frac{\sigma_1 - \sigma_3}{\gamma H}, \qquad P^* = \frac{\sigma_3}{\gamma H},$$

where σ_1, σ_3 is maximum and minimum components of the principal stress tensor, MPa; γ is the averaged weight of the overlying mine rocks, N/m^3; H is the mining depth, m.

3.3 Permeability of fractured rocks

The results of numerous experiments show that the permeability of the rock is a function of the acting stresses and has different meanings in different areas.

Permeability under elastic and uniform compression. Outside the zone of influence of mining, the rocks are in a state of compression with approximately equal components $\sigma_1 \approx \sigma_2 \approx \sigma_3$ ($Q^* < 0.6$). Compaction of rocks and overlapping of fissure-pore channels occur. The permeability filtration k is practically zero. The parameter P^* exceeds the threshold value $P^* = 0.1$, at which the deformation occurs in the regime of plastic or pseudoplastic flow [12]. With elastic deformation, the filtration properties of the medium do not significantly change [13]. We can assume that the zones of elasticity and uniform compression do not belong to the filtration area

$$k = 0 \text{ for } Q^* < 0.6;\ P^* > 0.25. \quad (8)$$

Permeability in the area of initial and intense cracking. For $\sigma_1 > \sigma_3$ ($0.6 < Q^* < 0.8$) microcracks begin to form. The increase in the permeability coefficient is insignificant, since this stage is characterized by the accumulation of single, non-interacting defects [12]. In this zone

$$k = k_{min} \text{ for } 0.6 < Q^* < 0.8. \quad (9)$$

Outside elasticity zone and when the ultimate strength is reached, which corresponds to the region of intense crack formation ($Q^* > 0.8$), uncontrolled crack growth occurs. At this stage, deformations rapidly increase due to the propagation of cracks and loosening of the rock [12]. With an increase in Q^*, the permeability coefficient increases by 2-3 orders of magnitude [14, 15]. A further increase in permeability beyond the ultimate strength occurs only due to the expansion of existing cracks. Using experimental data [16], the dependence of the permeability coefficient on Q^* was obtained

$$k = e^{0.26Q^* - 4.65} \text{ при } 0.8 < Q^* < 1.0. \quad (10)$$

Permeability in the rock destruction zone. When the rate of crack formation reaches a maximum, and the stresses of the ultimate strength of the rock, the process of macroscopic destruction begins. Destruction of geomaterials can be brittle, plastic or intermittent slip [12]. The permeability of the rock depends on this. The brittle fracture of the rock is characterized by an increase in deformations, loosening and, accordingly, the volume of the material. In the case of

plastic flow, material softening occurs without loosening it. Developing cracks are closed and their edges are tightly compressed. During compression deformation occurs with loosening for the condition P^*<0.1 [17]. In this case, the permeability coefficient takes the maximum values

$$k=k_{max} \text{ for } P^*<0.1;\ Q^*>1.0. \quad (11)$$

So the relationship between permeability coefficients in the disturbed rocks and geomechanical parameters is determined by relations (8)-(11).

3.4 An example of calculating methane filtration parameters for Pokrovskoye mine control conditions

Let us consider the rock area with 1st northern longwall (Fig. 3). The depth of mining is 570 m, the length of the longwall is 260 m. The thickness of the developed coal seam d_4 is 1.5 m. There are coal seam d_4^1 (0.15 m) 20 m above and coal seam d_4^2 (0.1 m) 38 m above.

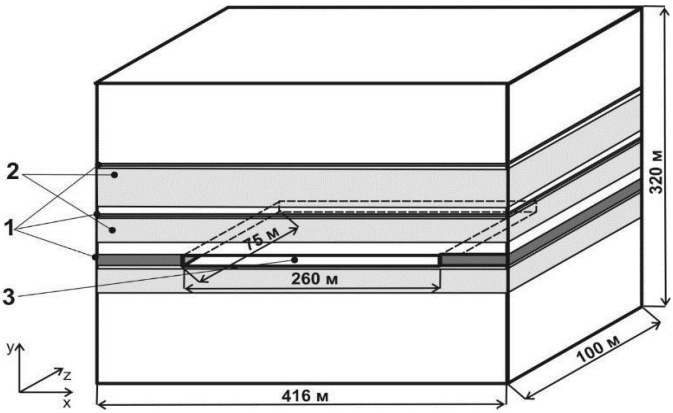

Fig. 3. Design model: *1* – the coal seams; *2* – the sandstones; *3* – the goaf

Potential sources of methane emissions are coal seams and sandstones. The natural gas content of coal is 20 m^3/ton, sandstones is 3.5 m^3/ton.

The fields of stress, permeability, distribution of methane pressure values and its filtration rates at each point of the studied area has been calculated. The calculations have been made for the wall advance speed V_{lw} 3, 6 and 9 m/day. The distribution of the relative

methane pressure p/p_0 in the central longitudinal section is shown in Fig. 4.

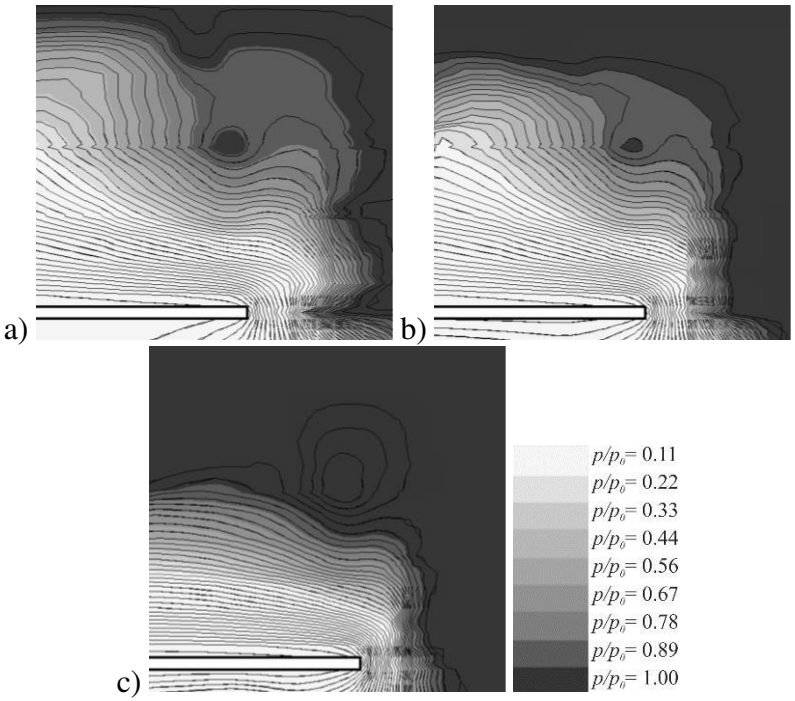

Fig. 4. Isobars of relative methane pressure in the central longitudinal section of the zone: *a* - V_{lw}=3 m/day; *b* - V_{lw}=6 m/day; *c*- V_{lw}=9 m/day

The p/p_0 distribution in the cross section z=50 m at a distance of 25 m behind the longwall face is shown in Fig. 5. It can be seen from the figures that in an untouched massif, the methane pressure remains equal to the pressure in the seam. Inside the filtration zone, the gas pressure is reduced. Methane partially moved to longwall atmosphere. With an increase in the speed of wall advance, the zone of reduced methane pressure decays, the rates of its desorption and filtration decrease as well. As a result, less methane is moved to the longwall.

a

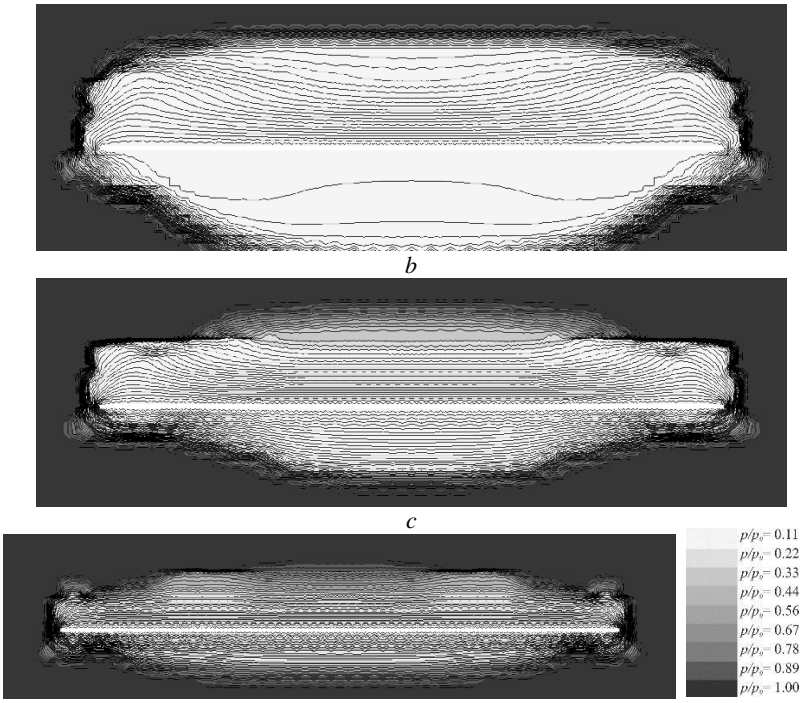

Fig. 5. Isobars of methane relative pressure in the cross section of the studied zone, z=50 m: *a* - V_{lw}=3 m/day; *b* - V_{lw}=6 m/day; c - V_{lw}=9 m/day

At V_{lw}=3 m/day in the roof of the longwall, two layers of gas-bearing sandstone and two coal seams will be inside of filtration area. The size of the sources of methane emission decreases with an increase in the speed of wall advance. At V_{lw}=12 m/day, the coal seam d_4^2 and the upper part of the gas-bearing sandstone are outside the filtration area. Its front border shifts closer to the longwall face. The volume of the filtration area at V_{lw} = 6 m/day decreases by 20 %, and at V_{lw}=9 m/day by 46 %.

The methane relative pressure (p/p_0) in the coal seams d_4^1 and d_4^2 at various speed of wall advance is shown on Fig. 6 и 7. Coordinate z of longwall face is 75 m.

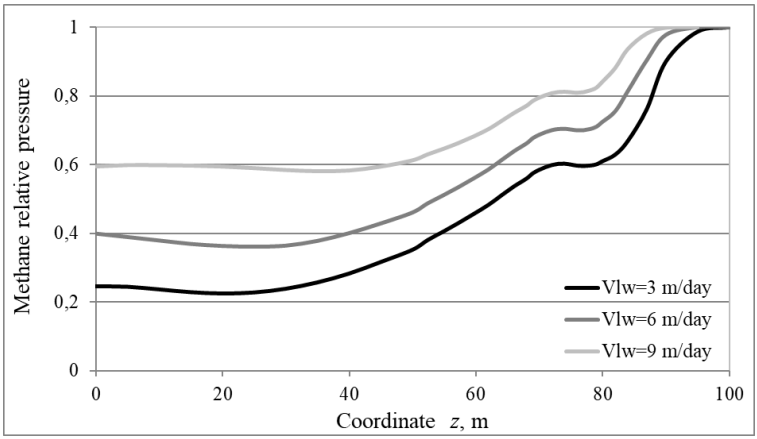

Fig. 6. Methane relative pressure in coal seam d_4^1 during its undermining

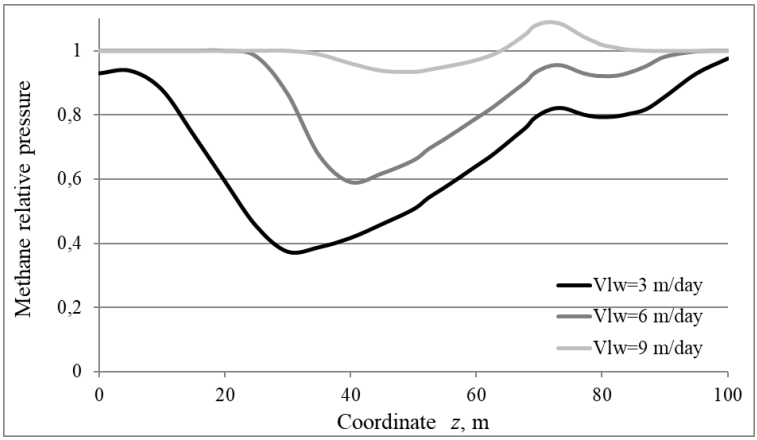

Fig. 7. Methane relative pressure in coal seam d_4^2 during its undermining

It can be seen from Figure 6, the methane pressure in seam d_4^1 is lower than in seam d_4^2. The coal seam d_4^1 is well degassed, unlike the one located above seam d_4^2. With an increase in the speed of wall advance, the relative residual pressure of methane increases from 0.25 to 0.6 (Fig. 6). The pressure in the upper coal seam at V_{lw}=9 m/day differs slightly from the pressure in the undisturbed seam (Fig. 7). Methane from it almost does not enter the longwall at such a speed of wall advance.

Increase in pressure with increase in the wall advance speed also slows down the process of desorption of methane from underworking coal seams.

Comparing the factual specific methane flowrates (Q/A, where Q – daily average methane inflow in longwall and adjoining mine workings, m^3; A – daily average coal production, t) in various mining sites with the calculated ones, we will see that specific methane flowrates decrease with increasing speed of wall advance in both cases (Fig. 8).

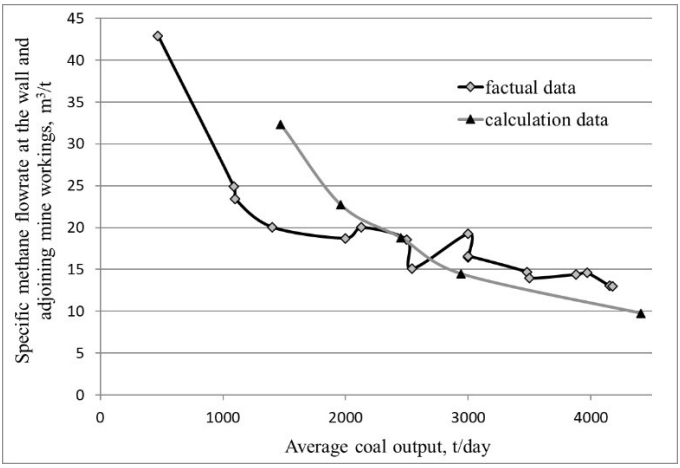

Fig. 8. Specific methane emission rate at the treatment area per ton of coal mined during coal production intensification

Thus, it was found that there is the reduction of methane specific emission at intensification of coal production from softly coal bed.

4 Conclusions

The length of the console hanging over the worked out longwall space is directly proportional to the thickness of the main roof and the modulus of elasticity of the rock, inversely proportional to the depth of mining and the degree of heterogeneity of the massif. With an increase in the speed of the wall advance, the length of this console increases linearly.

With an increase in the wall advance speed, the size of the blocks of destroyed sandstones increases, the process of formation of cracks in the roof rocks slows down. The size of the filtration area near the longwall is reduced. The front boundary of the filtration area shifts closer to the face. Remote sources of gas evolution completely or partially go beyond the filtration area. The residual pressure of methane in underworking gas-bearing rocks and coal seams increases. The cracking process slows down. For this reason, the emission of electrons from new cracks decreases, which activate methane molecules bound by the Van der Waals forces. This leads to a slowdown in methane desorption processes.

Thus, an increase in the speed of the wall advance can reduce the emission of methane in mine. However, due to the increase and redistribution of stresses in the array, the requirements for mechanized and drift supports increase. This should be taken into account when choosing the optimal operating conditions for the coal mine section.

Acknowledgements

The results are part of the program "Promoting the development of priority research areas" (KPKVK 6541230) of state funding for the National Academy of Sciences of Ukraine.

References

1. **Ilyashov, M.A., Agafonov, A.V., Kocherga, V.N., Bodnar, A.A., Skipochka, S.I., & Krukovskaya V.V.** (2009). The abundance of methane in mine workings during the intensive development of gently sloping coal seams. Geotechnical mechanics, 83, 14-25 [in Ukrainian].

2. **Bokiy, B.V., Kasimov, O.I., & Nazimko, I.V.** (2009). The effect of coal face movement speed on the stress-strain state and gas permeability of the massif. Coal of Ukraine, 11, 9-13 [in Ukrainian].

3. **Skipochka, S.I., Usachenko, B.M., & Kuklin, V.Yu.** (2006). Elements of geomechanics of coal and rock massif at high speeds of coal face movement. Dnepropetrovsk: Lira LTD [in Ukrainian].

4. **Skipochka, S.I., Usachenko, B.M., Ilyashov, M.A., Nazimko, V.V., & Mukhin, A.V.** (2004). The property of coal formation rocks in the process of their

destruction to exhibit additional desorption of bound methane molecules. Scientific discovery No. 275. Claimed on July 21, 2004; Priority 12/19/2002 [in Russian].

5. **Bulat, A.F., Skipochka, S.I., Palamarchuk, T.A., & Antsypherov, V.A.** (2010). Methanogeneration in coal seams. Dnepropetrovsk: Lira LTD [in Ukrainian].

6. **Barenblatt, G.I., Entov, V.M., & Ryzhyk V.M.** (1984). The movement of liquids and gases in natural seams. Moscow: Nedra [in Russian].

7. **Kush, O.A. & Kiriukov, V.V.** (2000). Perspectives for the development of gas-coal deposits in the Donbass. Geotechnical mechanics, 17, 23-29 [in Ukrainian].

8. **Shevelev, G.A.** (2000). Metano-intensity of sandstones containing coal seams. Geotechnical mechanics, 17, 204-207 [in Ukrainian].

9. **Malyshev, Yu.N., Trubetskoi, K.N., & Airuni, A.T**. (2000). Fundamental and applied methods for solving problems of coal seams methane. Moscow: Academy of Mining Sciences [in Russian].

10. **Basniev, K.S., Kochina, I.N., & Maksimov, V.M.** (1993). Underground hidromechanics. Moscow: Nedra [in Russian].

11. **Krukovska, V.V.** (2015). Simulation of coupled processes that occur in coal-rock massif during mining operations. Geotechnical Mechanics, 121, 48-99 [in Ukrainian].

12. **Vinogradov, V.V.** (1989). Geomechanics of massif condition control near mining. Kiev: Naukjva Dumka [in Ukrainian].

13. **Szlazak, J., & Szlazak, N.** (2004). Numerical determination of methane concentration in goaf space. Archives of mining sciences. Polish Academy of Sciences, Committee of Mining and Strata Mechanics Research Institute. Krakow, 49 (4), 587-599 [in Polish].

14. **Kulinich, V.S., & Kulinich, S.V.** (2000). The influence of the stress-strain state on the gas recovery of methane-bearing rocks. Geotechnical Mechanics, 17, 152-156 [in Ukrainian].

15. **Stavrogin, A.N., & Protosenia, A.G.** (1985). The strength of the rocks and of the workings stability at great depths. Moscow: Nedra [in Russian].

16. **Kulinich, V.S., Perepelitsa, V.G., Kurnosov, S.A., Ivanchishin, S.Ya., Shumeiko, A.M., & Kulinich, S.V**. (2003). The gas permeability of rocks in a multicomponent field of compressive stress. Geotechnical Mechanics, 42, 18-24 [in Ukrainian].

17. **Li S.P., & Wu D.X.** (1997). Effect of confining pressure, pore pressure and specimen dimension on permeability of Yinzhuang sandstone. Int. J. Rock Mech. Min. Sci., 34(3/4), 435-441.